Available online at www.sciencedirect.com
SCIENCE DIRECT®
Journal of Colloid and Interface Science 281 (2005) 275–284
JOURNAL OF Colloid and Interface Science
www.elsevier.com/locate/jcis

Adsorption and precipitation of an aminoalkylphosphonate onto calcite

Amy T. Kan *, Gongmin Fu, Mason B. Tomson

Department of Civil and Environmental Engineering, Rice University, Houston, TX, USA

Received 14 April 2004; accepted 12 August 2004

Available online 22 September 2004

Abstract

The mechanism of nitrilotris(methylenephosphonic acid) (H_6NTMP)/calcite reaction was studied with a large number of batch experiments where phosphonic acid was neutralized with 0 to 5 equivalents of NaOH per phosphonic acid and the concentration ranged from about 10 nmol/L to 1 mol/L. It is proposed that the phosphonate/calcite reactions are characterized in three steps. At low phosphonate concentration (<1 µmol/L NTMP concentration), the phosphonate/calcite reaction can be characterized as a Langmuir isotherm. At saturation, only ∼7% of the calcite surface is covered with phosphonate; presumably these are the kinks, step edges, or other imperfect sites. At higher phosphonate concentrations, the attachment is characterized by calcium phosphonate crystal growth to a maximum of four to five surface layer thick, with solid phase stoichiometry of $Ca_{2.5}$HNTMP and a constant solubility product of $10^{-24.11}$. After multiple layers of phosphonate are formed on the calcite surface, the solution is no longer at equilibrium with calcite. Further phosphonate retention is probably due to mixed calcium phosphonate solid phase formation at lower pH and depleted solution phase Ca conditions. The proposed mechanism is consistent with phosphate/calcite reaction and can be used to explain the fate of phosphonate in brines from oil producing wells and the results are compared with two oil wells.
© 2004 Elsevier Inc. All rights reserved.

Keywords: Phosphonates; Calcite; Adsorption; Precipitation; Scale inhibition

1. Introduction

Aminoalkylphosphonates, e.g., nitrilotris(methylenephosphonic acid) (NTMP), are widely used in a broad variety of applications. Their ability to prevent precipitation of calcium and barium salts at substoichiometric concentrations (threshold inhibition) finds wide application in water treatment, water conditioning, cooling tower and oil and gas wells. These materials are also used as corrosion inhibitors, in industrial cleaning, metal finishing, and agrochemical applications.

In matured oil and gas fields, approximately 10 barrels of salt water is produced per barrel of oil [1]. Produced brines tend to precipitate calcite and sulfate scale and these aminoalkylphosphonates are the most commonly used chemicals for scale inhibition. Phosphonate is typically applied in oil wells via inhibitor squeezes, where phosphonate solutions (0.5–20% wt/vol) of various acidity are pumped into a producing formation and allowed to react. A large portion of phosphonate is retained in the formation. Even though phosphonates are widely used in industries, their interaction with soil or formation rock is still poorly understood. The objective of this paper is to quantify the interaction of phosphonates with calcite and relate phosphonate retention and release from formation material.

The chemical/physical properties of phosphonates bear many similarities to those of orthophosphate [2]. Therefore, phosphate/calcite interaction chemistry may provide clues to phosphonate/calcite interaction. In calcareous soil, the predominant sorption site for phosphate is calcite. At low concentrations, the adsorption of phosphate and phosphonate on calcite has been studied in detail [3–15]. Several in situ atomic force microscope (AFM) [3–5,15] and X-ray photoelectron spectroscopy [6] studies showed that phosphonate and phosphate are adsorbed to the growth sites (kink

* Corresponding author.
E-mail address: atk@rice.edu (A.T. Kan).

0021-9797/$ – see front matter © 2004 Elsevier Inc. All rights reserved.
doi:10.1016/j.jcis.2004.08.054

site, step edges, and terraces) and further growth of calcite is therefore inhibited. At low phosphate concentrations, the phosphate adsorption isotherm is very strong and can be described by a Langmuir model [7]. In the presence of Ca^{2+}, the adsorption of phosphate and phosphonate to vaterite, calcite, barite, and goethite is much stronger than in the absence of Ca^{2+} [8–13]. Suzuki et al. [10] proposed the adsorbed species to be $Ca_3(PO_4)_2^{\pm 0}$ at low phosphate concentration and $CaHPO_4^{\pm 0}$ at higher concentrations. However, the adsorption of the calcium phosphate ion pairs onto the calcite surface is not distinguishable from separate adsorption of calcium and phosphate ions. Tomson et al. [12] proposed that the primary driving force for phosphonate adsorption is related to simple hydrophobic repulsion from solution of a macroneutral molecule and not, as is generally presumed, some specific phosphonate–surface interaction.

At high phosphate concentrations sorption occurs in two steps, the fast chemisorption of phosphate to a limited number of specific surface sites followed by the spontaneous crystal growth on the cluster of surface phosphate ions (heteronuclei) [8,16]. Calcium phosphate crystals, e.g., amorphous calcium phosphate [17], dicalcium phosphate [7] or octacalcium phosphate [16] and/or calcium–carbonate–phosphate surface complexes [18], have been identified on calcite surfaces. Several authors have proposed the phosphate calcite reaction to be a surface precipitation of brushite that slowly transforms to the more stable octacalcium phosphate [19]. Stumm and Leckie [20] postulate that the reaction occurs in three steps: (1) chemisorption of phosphate to form amorphous calcium phosphate; (2) slow transformation of the amorphous calcium phosphate to hydroxyapatite; and (3) crystal growth of apatite. Hinedi et al. [21] observed that the sorbed phosphate is not in the form of hydroxyapatite or amorphous calcium phosphates at less than 0.037 µmol PO_4/m^2 calcite level. An apatitic-like phase formed at a phosphorus sorption level of 0.15–1.67 µmol PO_4/m^2 calcite. At higher phosphate levels, both apatite and brushite were detected.

The precipitation of phosphonate with calcite at high phosphonate concentration is much less well known. According to a recent study by Jonasson et al. [6], a calcium diethylenetriaminepenta(methylene phosphonate) solid phase was uniformly distributed on calcite surface at low phosphonate concentrations. When phosphonate concentration is sufficiently high, an intimate mixture of submicrometer-sized crystals of calcite and calcium phosphonate precipitates is observed [6]. In this paper, the interaction of NTMP with calcite over a wide range of phosphonate concentration and acidity has been studied.

2. Materials and methods

Phosphonate used in this study is a technical grade H_6NTMP (Dequest 2000, Solutia Inc., 299 MW) (Fig. 1). It contains 50% phosphonate and 0.19 mol excess mineral acid

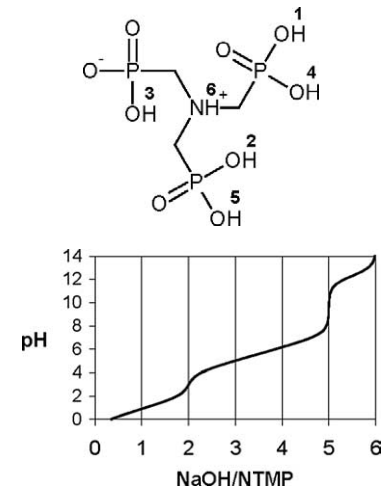

Fig. 1. Chemical structure and acid/base potentiometric titration of nitrilotris(methylenephosphonic acid), NTMP.

(HCl) per mole of phosphonic acid [22]. All other chemicals used in this study are reagent grade. Stock solutions of phosphonate (∼0.001 to 0.1 M) were prepared in 1 M NaCl solution. From 0 to 5 equivalents of NaOH per mole phosphonate was also added to the stock solutions. A typical acid/base titration curve of NTMP is shown in Fig. 1. There are five protons associated with the phosphonate ligands. The phosphonate protons are completely dissociated when five equivalents of NaOH is added to the phosphonate stock solution; the sixth proton equivalent is on the very basic nitrogen ($pK_a = 10^{12.3}$) and does not dissociate at pH values commonly encountered.

^{14}C-radiolabeled calcite was prepared in order to facilitate carbonate analyses with high precision. The [^{14}C] calcite was synthesized in the laboratory by slowly adding a $CaCl_2 \cdot 2H_2O$ (1.4 m) solution into a $^{14}C/^{12}C$ $NaHCO_3$–Na_2CO_3 solution with constant stirring. The $^{14}C/^{12}C$ $NaHCO_3$–Na_2CO_3 solution contained equal molality of $NaHCO_3$ and Na_2CO_3 at a total carbonate concentration of 1.33 m and a specific ^{14}C radioactivity of 0.49 mCi/mol carbonate. During mixing, the solution pH was controlled at pH 8.3 by titrating with a small volume of 5 m NaOH solution. The initial precipitate was then boiled and washed with deionized water four times over three days to allow for Osward ripening. Finally the [^{14}C] calcite was dried under vacuum. The average [^{14}C] calcite solid particle diameter is ∼18 µm. The crystallography of [^{14}C] calcite has been confirmed with X-ray diffraction, where the X-ray diffraction peaks were detected at 2θ of 23.28, 29.58, 36.02, and 39.28 and at a wavelength of 1.5418 A. According to Bragg equation [23], the 2θ values corresponded to the interplanar distances (d spacing) of 3.02 A (100%), 2.49 A (13%), 2.29 A (12%), and 3.81 A (7.7%) (Fig. 2). The referenced calcite d spacing are 3.04 (100%), 2.29 (18%), 2.10 (18%), and 3.86 (12%) (JCPDS record 5-0584) and aragonite d spacing are 3.40 (100%), 1.98 (65%), 3.27 (52%), and 4.212 (2%) (JCPDS record 5-0453) [24]. Clearly, the XRD

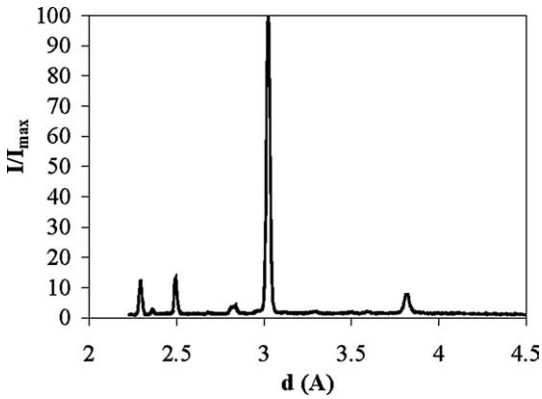

Fig. 2. X-ray diffractive pattern of the ^{14}C calcite prepared in the laboratory.

spectrum resembles calcite instead of aragonite. The SEM picture also showed typical calcite hexagonal morphology instead of the orthorhombic shape of aragonite (see Fig. 6 below). In addition, controlled solubility experiments have confirmed that the solid is calcite (see Table 3).

Batch adsorption experiments were run in closed bottles where calcite was added to an initially calcium free phosphonate solutions at a solid to solution ratio of 0.02 g/ml. The samples were mixed in a horizontal shaker bath at 70 °C for 2 days. After the equilibrium time, the samples were centrifuged at 5000 rpm for 15 min and the supernatant solutions were analyzed for total carbonate (TCO_3), total calcium (TCa) and total phosphonate ($TNTMP_{final}$) concentrations. The solid phase phosphonate concentrations ($TNTMP_{ads}$) were calculated from the difference of initial ($TNTMP_{init}$) and final ($TNTMP_{final}$) solution phase phosphonate concentrations. In Table 1 are listed eight groups (I–VIII) of experimental conditions. Exp. I is the control group of experiments to measure the solubility of [^{14}C] calcite in 1 M NaCl. Neither phosphonate nor NaOH was added to the sample bottles. For Exps. II–VIII, phosphonate solutions, neutralized with 0 to 5 equivalents of NaOH per phosphonate, were used. In each experimental group, between 7 and 32 individual experiments were run at different phosphonate concentrations. In Table 1, the ranges of initial phosphonate concentrations ($TNTMP_{init}$) are listed in column 3, the ranges of NaOH concentrations are listed in column 4, and the equivalents of net base (Na^+–Cl^-) per phosphonate are listed in column 5. In Exp. VIII, reagent grade calcite was used instead of [^{14}C] calcite. Other than the difference in calcite solids, Exps. VI and VIII are similar in experimental condition and therefore, allow the comparison of phosphonate sorption to the two different calcite samples. Exp. VIII was also done to test the adsorption at much lower phosphonate concentration range. For these low phosphonate experiments ($TNTMP_{init} = 8.5 \times 10^{-4}$–$4 \times 10^{-3}$ mM), it is difficult to analyze the solution phase phosphonate concentration; in these experiments, the solid phase phosphonate concentrations yield better stoichiometries. First, a portion of the calcite solid was separated by centrifugation with an Ultrafree-MC centrifugal filter (Millipore). The solid was then dissolved in acid and analyzed for the phosphonate content. The solution phase phosphonate concentrations were then calculated from the difference between $TNTMP_{init}$ and solid phase concentrations.

Most calcium and phosphonate concentrations were analyzed by ICP. HACH colorimetric method was used to analyze low phosphonate concentrations. The total carbonate in solution was measured by scintillation counting. The solution pH was measured by a Ross combination pH electrode. X-ray diffraction (XRD) spectra was taken using a Siemens platform-model general area detector diffraction system (GADDS). The BET surface area for the reagent grade calcite is 0.45 m^2/g. The surface area of the ^{14}C-labeled calcite is estimated to be 0.75 m^2/g. Scanning electron microscopic analysis with energy dispersive detection were done on the Au-coated [^{14}C] calcite and selected solid samples of experiment VIII using a high resolution (2 nm) thermal field emission electron microscope equipped with an EDAX X-ray system for elemental analysis (FEI XL-30 environmental scanning electron microscope).

Data interpretation

The authors have published conditional stability constants for NTMP at 0–3 M ionic strength and 25–90 °C [22]. Analogous to calcium phosphate, three calcium NTMP solid phases of different stoichiometries, namely, (1) acidic $Ca_{1.25}H_{3.5}NTMP$ [25], (2) amorphous $Ca_{2.5}HNTMP$, and (3) crystalline $Ca_{2.5}HNTMP$ [22], and several other metal phosphonate salts have been identified by the authors' re-

Table 1
List of the experimental parameters of nine phosphonate/calcite experiments

Exp. group No.	Number of experiments	Calcite	$TNTMP_{init}$ (mM)	NaOH (mM)	$(Na^+ - Cl^-)/TNTMP_{init}$ (mol/mol)
I	8	^{14}C labeled	0	0	0
II	8	^{14}C labeled	0.013–12.5	0.0	−0.19
III	7	^{14}C labeled	0.013–12.7	0.013–12.8	1.00
IV	8	^{14}C labeled	0.013–25.3	0.025–49.2	1.95
V	9	^{14}C labeled	0.013–25.3	0.038–75.7	2.99
VI	9	^{14}C labeled	0.012–25.3	0.049–100.9	3.98
VII	9	^{14}C labeled	0.013–25.1	0.065–125.3	4.99
VIII	32	^{12}C (reagent gr.)	8.54×10^{-4}–1019	2.25×10^{-3}–4101	4.00

Table 2
Conditional stability constants and solubility products (at 1 M I and 70 °C)

Cation	Equilibrium	Log K	Ref.
H^+	$H^+ + NTMP^{6-}$	12.3	[23]
	$H^+ + HNTMP^{5-}$	6.73	
	$H^+ + H_2NTMP^{4-}$	5.58	
	$H^+ + H_3NTMP^{3-}$	4.44	
	$H^+ + H_4NTMP^{2-}$	1.80	
	$H^+ + H_5NTMP^{-}$	0.30	
Ca^{2+}	$Ca^{2+} + HNTMP^{5-}$	2.82	
	$Ca^{2+} + CaHNTMP^{3-}$	1.69	
	$Ca^{2+} + Ca_2HNTMP^{-}$	0.56	
	$Ca^{2+} + H_2NTMP^{4-}$	2.25	
	$Ca^{2+} + CaH_2NTMP^{2-}$	1.13	
	$Ca^{2+} + H_3NTMP^{3-}$	1.69	
	$Ca^{2+} + CaH_3NTMP^{-}$	0.56	
	$Ca^{2+} + H_4NTMP^{2-}$	1.13	
	$Ca^{2+} + H_5NTMP^{-}$	0.56	
H^+	$H^+ + OH^-$	12.55	
	$H^+ + CO_3^-$	9.13	
	$H^+ + HCO_3^-$	5.94	

Solid phase	Equilibrium	pK_{sp}	Ref.
$CaCO_3$	$Ca^+ + CO_3^{2-}$	6.96	[30]
$Ca_{2.5}HNTMP_{am}$	$2.5Ca^{2+} + H^+ + Phn^{6-}$	21.31	[23]
$Ca_{2.5}HNTMP_{low\ solubility}$	$2.5Ca^{2+} + H^+ + Phn^{6-}$	23.46	[23]
$Ca_{2.5}HNTMP_{cr}$	$2.5Ca^{2+} + H^+ + Phn^{6-}$	24.11	This study
$Ca_5(PO_4)_3OH$	$5Ca^{2+} + 3PO_4^{3-} + OH^-$	48.79	[31]

search group [2,22,25–29]. He et al. [30] published a set of conditional stability constants for carbonate and calcium carbonate salt. The conditional solubility product of hydroxyapatite ($Ca_5(PO_4)_3OH$) was calculated from the thermodynamic solubility product of hydroxyapatite [31] and the Pitzer activity coefficients for Ca^{2+} and PO_4^{3-} [32]. These equilibrium constants at 70 °C and 1 M ionic strength were listed in Table 2. The following charge balance and mass balance equations were used to calculate the solution pH, $[Ca^{2+}]$, $[CO_3^{2-}]$, and $[NTMP^{6-}]$ concentrations; the following four equations were solved iteratively by a Newton–Raphson procedure:

$$[Na^+] - [Cl^-] = 6[NTMP^{6-}] + \sum_{i=1}^{6}\sum_{j=0}^{(6-i)/2}(6-i-2j)[Ca_jH_iNTMP^{6-i-2j}] + [OH^-] - [H^+] - 2[Ca^{2+}], \quad (1)$$

$$TNTMP = [NTMP^{6-}] + \sum_{i=1}^{6}\sum_{j=0}^{(6-i)/2}[Ca_jH_iNTMP^{6-i-2j}], \quad (2)$$

$$TCa = [Ca^{2+}] + \sum_{i=1}^{6}\sum_{j=1}^{(6-i)/2} j[Ca_jH_iNTMP^{6-i-2j}], \quad (3)$$

$$TCO_3 = [H_2CO_3] + HCO_3^- + CO_3^{2-}, \quad (4)$$

where [ ] refer to molar concentrations. Note that pH values calculated by these equations are generally in excellent agreement with measured pH as shown in Kan et al. [33,34]. The negative logarithmic $Ca_{2.5}HNTMP$ and $CaCO_3$ ion products (pIP) were then calculated and compared with the reported solubility products of calcium carbonate and the three calcium phosphonate salts,

$$pIP_{calcite} = -\log\ [Ca^{2+}]\ CO_3^{2-}, \quad (5)$$

$$pIP_{Ca2.5HNTMP} = -\log\ [Ca^{2+}]^{2.5}\{H^+\}[NTMP^{6-}], \quad (6)$$

where $\{H^+\}$ is the hydrogen ion activity, $\{H^+\} = 10^{-pH}$.

3. Results and discussion

In Table 3 are listed the equilibrium solution compositions of Exps. I–VIII, pH, pIP for calcite and $Ca_{2.5}HNTMP$. Note that the solution matrix contained 1 M NaCl in all experiments. Therefore, small changes in solution composition, due to precipitation/dissolution reactions, change the overall ionic strength only a few percentage. Such small changes in ionic strength have a negligible effect on solution phase ion activity [2,22,27]. In Fig. 3 are plotted the phosphonate solid phase concentrations vs solution phase concentrations of Exps. II–VIII. The adsorption of phosphonate to the reagent grade calcite (Exp. VIII) is very similar to that of the [^{14}C] calcite (Exp. VI). The data in Fig. 3

Table 3
List of the range of eight groups of phosphonate/calcite experimental results

Exp. group No.	Total carbonate concentration (TCO_3) (mM)	Total calcium concentration (TCa) (mM)	Total NTMP concentration ($TNTMP_{final}$) (mM)	pH[a]	$pIP_{calcite}$	$pIP_{Ca2.5HNTMP}$
I	0.55–5.69	0.48–0.55	0.0	8.96–8.98	7.06–6.86	–
II	0.50–23.1	0.47–7.21	0.054–3.45	8.82–4.84	7.06–9.27	26.3–23.2
III	0.53–22.9	0.47–5.23	0.0024–3.94	8.88–5.65	7.04–7.98	26.4–22.3
IV	0.53–23.1	0.52–4.59	0.0030–9.27	9.02–6.46	6.92–7.26	26.2–22.1
V	0.52–19.7	0.54–4.07	0.0018–12.1	9.09–8.53	6.88–5.63	26.4–22.5
VI	0.51–29.5	0.32–0.73	0.0014–11.7	9.05–9.10	6.92–5.90	26.5–24.4
VII	0.55–5.69	0.50–1.89	0.0027–19.4	8.98–10.87	6.94–6.08	26.3–23.6
VIII	–	0.60–68.3	2.21×10^{-5}–901	9.41–6.29[b]		28.2–21.9

[a] Calculated from Eqs. (1)–(4).
[b] Measured pH.

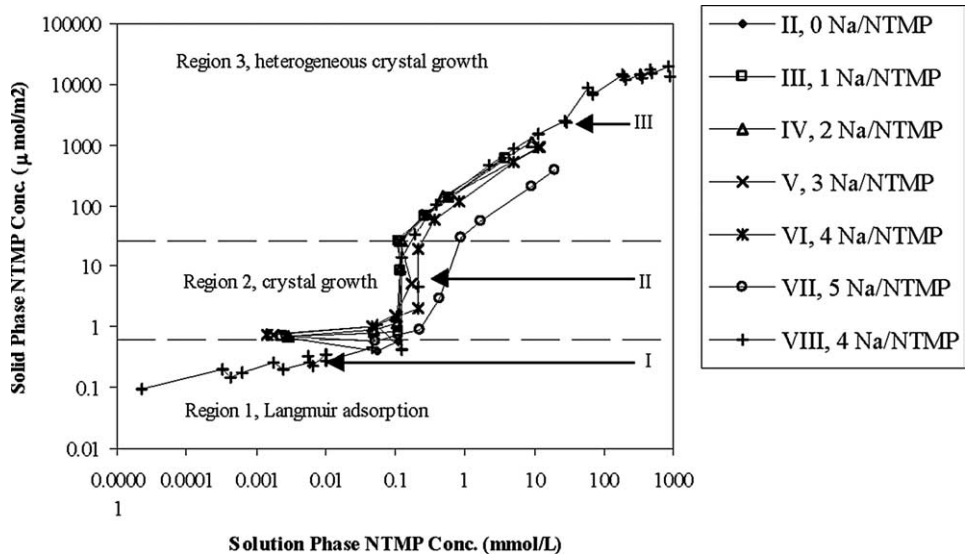

Fig. 3. Plots of solid vs solution phase phosphonate concentrations for Exps. II–VIII where the phosphonate solutions were neutralized with NaOH at a NaOH/Phosphonate molar ratio of 0–5 Na/NTMP.

clearly deviate from typical adsorption isotherms, but similar isotherms have been reported for the adsorption of phosphate to calcite [19]. The data in Fig. 3 can be divided into three regions. In region 1 ($TNTMP_{ads} < 0.6$ μmol/m^2), the solid phase concentration increased by less than one order of magnitude while the phosphonate concentration increased by over three orders of magnitude. It is proposed that strong phosphonate adsorption occurred in region 1 (see below). In region 2, the solid phase concentration varied between 0.6 and 26 μmol/m^2 while NTMP solution concentrations remained relatively constant (0.1–0.2 mmol/L). In this region, precipitation appeared to govern the solid reaction. In region 3, the isotherms follow a more normal shape with increasing amount of phosphonates reacting with the surface as the amount in solution increased. Three solid samples from Exp. VIII (labeled as A, B, C) were analyzed by SEM/EDAX surface analyses (see Fig. 6 and discussion below). Detailed analyses of these three regions of data are discussed below.

It is proposed that the attachment of low concentrations of phosphonate to calcite is by a Langmuir type adsorption, similar to the adsorption of phosphate to calcite. For Exps. II–VII, all data in region 1 of the isotherm appeared to reach the plateau level. At 1 M ionic strength, the electrostatic interaction between surface sites should be negligible and the use of the Langmuir isotherm is justifiable. Only when the phosphonate concentrations were lowered (as in Exp. VIII) could the shape of the adsorption curve be evaluated. In Fig. 4 is plotted the solid phase phosphonate concentrations vs the solution phase concentrations of the data of Exp. VIII in region 1. The data appear to follow a Langmuir isotherm at $TNTMP_{final} < 0.007$ mM, as shown in Fig. 4. The adsorption data can be fitted with a Langmuir

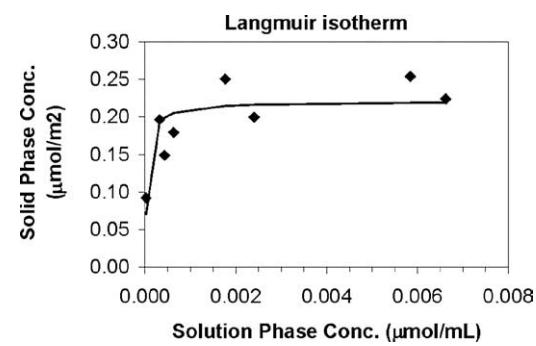

Fig. 4. Plot of the adsorption isotherm of phosphonate to calcite at $TNTMP_{final} = 0$–0.12 mM. The data are from Exp. VIII. The inserted plot is the adsorption isotherm at $TNTMP_{final} = 0$–0.0008 mM and the Langmuir isotherm fit to the data.

isotherm,

$$q(\mu\text{mol/m}^2) = \frac{0.22(\mu\text{mol of NTMP/m}^2)}{1 + 2.14 \times 10^5 C} \times 2.14 \times 10^5 (\text{mL/m}^2) C(\mu\text{mol/mL}),$$

$$r = 0.82, \tag{7}$$

where units have been selected to facilitate comparisons.

The Langmuir capacity is 0.22 ± 0.02 μmol of NTMP/m^2. The Langmuir adsorption slope is $2.14 \times 10^5 \pm 1.40 \times 10^5$ ml/m^2. The low correlation coefficient and large standard deviation of the adsorption slope is partly due to the paucity of low concentration data ($TNTMP_{final} < 0.0001$ mM). However, these data are consistent with literature adsorption data for ethylenediamine-N,N,N',N'-tetrakis-(methylenephosphonic acid) with calcite [35] and for NTMP with goethite [36] (see Table 4). For the purpose of comparison, the concentration units in Table 4 are in terms of phosphorus concentrations. Furthermore, the adsorption maximum is very similar in magnitude to the adsorption of

Table 4
Comparison of the Langmuir adsorption plateau of phosphate/calcite, phosphonate/calcite, and phosphonate/goethite reactions at the adsorption regime

Adsorbent (SSA)	Adsorbate	Ca concentration (mM)	pH	Range of solution phase[a] concentration at plateau (μmol P/L)	Solid phase[a] concentration at plateau (μmol P/m^2)	Ref.
Calcite (0.5 m^2/g)	Orthophosphate	1	7.4	1.59–25	0.5	[19]
Calcite (0.37 m^2/g)	Orthophosphate	0.6	9.0	6–10	1.24	[38]
Calcite (22 m^2/g)	Orthophosphate	0.7	7.39	16.7	0.15	[21]
Calcite (0.14 m^2/g)	Ethylenediamine-N,N,N',N'-tetrakis (methylenephosphonic acid)	1 and 5	9.0	4–400	0.45	[36]
Calcite (0.45 m^2/g)	NTMP	0.6	9.0	3–20.4	0.66	This study
Goethite (47.6 m^2/g)	NTMP	1	7.2	15–36	3.33	[13]

[a] For comparison purpose, the units are micromoles of phosphorus per unit volume or per surface area. NTMP has three phosphorus per mole and ethylenediamine-N,N,N',N'-tetrakis(methylenephosphonic acid) has four phosphorus per mole.

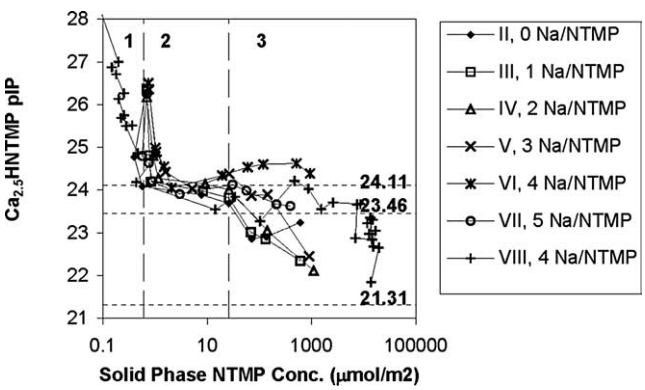

Fig. 5. Plot of the negative logarithm of $Ca_{2.5}$HNTMP ion products ($pIP_{Ca_{2.5}HNTMP}$) vs solid phase phosphonate concentrations of Exps. II–VIII (0–5 Na/NTMP).

orthophosphate to calcite [19,21,37]. In Table 4 are listed the literature reported Langmuir adsorption maximum and that observed in this study. Also listed in column 5 of Table 4 is the wide range of solution phase phosphorus concentrations that this adsorption maximum was observed. The adsorption maximum is very similar for all the calcite data (Table 4, column 6, average of top four rows is 0.6 ± 0.4 μmol of P/m^2 vs 0.66 μmol of P/m^2 from this study). Assuming a surface area of 20 Å^2 per Ca atom on the rhombohedral cleavage face of calcium carbonate, the number of calcium per unit area would be equivalent to 8.3 μmol/m^2 [21]. At the adsorption plateau, approximately 7.2% of the surface sites are covered by phosphorus molecules of either phosphonate or phosphate. Presumably this is the number of kinks, step edges, or other imperfect sites that is available for sorption [39]. The literature reported adsorption maximum is five times larger for goethite than for calcite.

In Fig. 5 is plotted the $pIP_{Ca_{2.5}HNTMP}$ vs the phosphonate solid phase concentration for the data of Exps. II–VIII. Also plotted in Fig. 5 are three constant pIP lines at 24.11, 23.46, and 21.31 pIPs. The 23.46 and 21.31 lines correspond to the solubility products of two previously identified calcium NTMP salts. As would be expected, the solution in region 1 has a high pIP at low phosphonate concentrations. When the phosphonate concentration increased, the $pIP_{Ca_{2.5}HNTMP}$ reduced continuously in region 1, as the phosphonate in solution is approaching a solubility limit. In region 2, the $pIP_{Ca_{2.5}HNTMP}$ is randomly distributed around a constant pIP = 24.11. Interestingly, the 4.5th root of this pIP is equal to 5.34. The 9th root of the solubility product of hydroxyapatite is 5.42, which is remarkably similar to the 4.5th root of $pIP_{Ca_{2.5}HNTMP}$. Assuming that the number of reactive sites equals 8.3 μmol/m^2, approximately 4–5 molecular layer of phosphonate is formed at this constant $Ca_{2.5}$HNTMP ion product of about 24.11. In region 3, the $pIP_{Ca_{2.5}HNTMP}$ for the more acidic phosphonate experiments (0–3 Na/NTMP) gradually decreases, while phosphonate in the 4–5 Na/NTMP experiments continue to precipitate up to about 1000 μmol/m^2 wherein the solution phase $pIP_{Ca_{2.5}HNTMP}$ remains nearly constant at 24.11. At >1000 μmol/m^2 concentration, the pIP of Exp. VIII (4 Na/NTMP) eventually decreases toward the amorphous calcium phosphonate solubility product (21.31).

In Fig. 6 are shown the SEM pictures of (a) a pure [^{14}C] calcite, (b–d) three selected solid samples from Exp. VIII (data points A–C of Fig. 3), and (e) a pure $Ca_{2.5}$HNTMP solid phase prepared by Frostman [40] using the procedure outlined in Frostman et al. [22]. The three solid samples are taken from regions 1–3 of Exp. VIII. As shown in Fig. 6a, the [^{14}C] calcite morphology is characteristic as calcite, not aragonite. Figs. 6b and 6c are calcite samples from Exp. VIII with low (region 1, A) to medium (region 2, B) range of phosphonate adsorbed. The morphology of the solid phases is not noticeably different from that of pure calcite. EDAX analyses of the solid phases in Figs. 6b and 6c showed a Ca/P ratio of ∼11, indicating a trace level of phosphorus on the surface of the calcite. However, the EDAX analysis at such low P intensity is not quantitatively reliable, due to the low

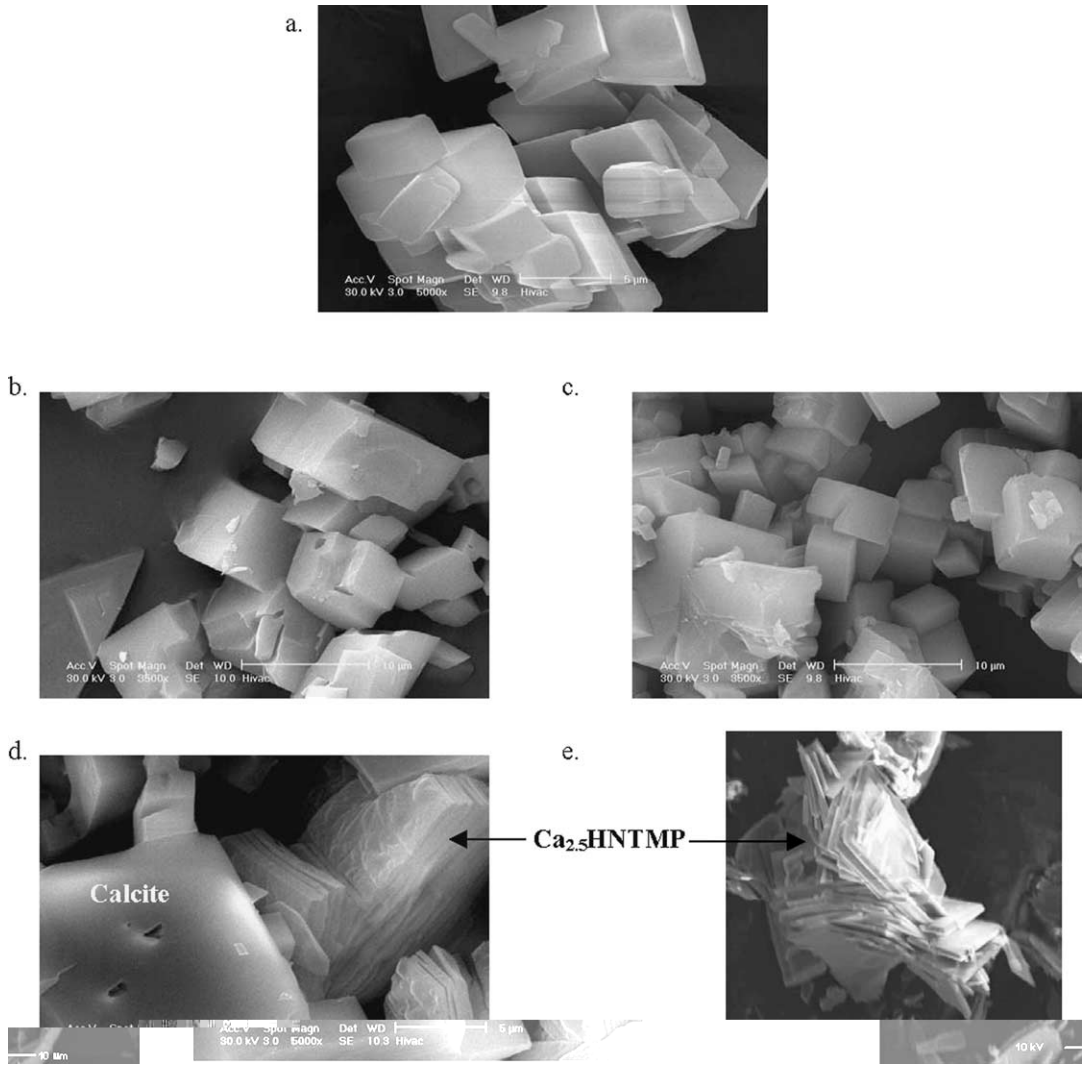

Fig. 6. Scanning electron micrographs of gold plated samples of (a) a pure ^{14}C calcite, (b–d) three solid phases from Exp. VIII, and (e) a pure $Ca_{2.5}HNTMP$ crystalline phase prepared by Frostman. The experimental conditions of Exp. VIII are shown in Table 1. The samples of (b)–(d) are taken from Exp. VIII as shown in Fig. 3, with labels A, B, and C.

phosphorus signal and spectrum interference from the gold coating. The SEM picture of the solid sample from region 3 (Fig. 6d) showed both calcite particles and particles that have a distinctively different morphology than calcite (thin platted structure). The morphology of the thin platted structure is similar to that of a pure $Ca_{2.5}HNTMP$ crystalline solid phase prepared by Frostman using ultrafiltration technique [39] (Fig. 6e). EDAX analysis of the pure $Ca_{2.5}HNTMP$ crystalline solid phase is not available, but EDAX analysis of this thin platted solid phase in Fig. 6d yields a Ca/P ratio of ∼1.15, which is slightly higher that expected for the $Ca_{2.5}HNTMP$ stoichiometry (Ca/P = 0.83). The higher Ca/P ratio may be due to interference from calcite or due to the semiquantitative nature of the EDAX analysis.

In Fig. 7 is plotted the $pIP_{Calcite}$ vs solid phase phosphonate concentrations of Exps. II–VII and the horizontal dotted line is at constant pIP = 6.96, the conditional solubility product of calcite. In region 1, the solution is ap-

Fig. 7. Plot of the negative logarithm of calcite ion products ($pIP_{Calcite}$) vs solid phase phosphonate concentrations of Exps. II–VII (0–5 Na/NTMP).